

Directed Percolation Universality in Asynchronous Evolution of Spatio-Temporal Intermittency

Juri Rolf,* Tomas Bohr,[†] and Mogens H. Jensen[‡]

Niels Bohr Institute and Center for Chaos and Turbulence Studies, Blegdamsvej 17, DK-2100 Ø, Denmark

(July 4, 2019)

Abstract

We present strong evidence that a coupled-map-lattice model for spatio-temporal intermittency belongs to the universality class of directed percolation when the updating rules are *asynchronous*, i.e. when only one randomly chosen site is evolved at each time step. In contrast, when the system is subjected to parallel updating, available numerical evidence suggest that it does not belong to this universality class and that it is not even universal.

PACS numbers: 05.45.+b, 05.70.Jk, 47.27.Cn

Typeset using REVTEX

*Electronic Address: rolf@nbi.dk

[†]Electronic Address: tbohr@nbi.dk

[‡]Electronic Address: mhjensen@nbi.dk

The onset of spatio-temporal intermittency is a common phenomenon of many extended systems ranging from models based on coupled-map-lattices [1,2] to various experiments in convection [5,6] and in the “printers instability” [7]. A particular elegant coupled-map-lattice (CML) showing spatio-temporal intermittency was introduced some years ago by Chaté and Manneville [2]. This CML employs individual maps that can be in two very different states: either in a chaotic (or “turbulent”) state or in a “laminar” state. For a single map the laminar state is “absorbing”: once the motion is in the laminar state it cannot escape. For the coupled system, one observes interesting dynamical patterns of turbulent patches penetrating into a laminar state, and because of the strong fluctuations, this has been called [1] spatio-temporal intermittency (STI). Once the system is in a pure laminar state, it cannot escape: this is an absorbing state of the full spatially coupled system. These properties of the STI led Pomeau [4] to conjecture that the critical properties at the onset of STI should be governed by the exponents of directed percolation. The turbulent spots of the dynamics in a space-time plot percolate through the system in a manner very similar to the connected bonds in directed percolation (DP), which also has an absorbing state. Subsequent extensive numerical studies and scaling arguments [3,1,9] did not show agreement with this conjecture. On the contrary, it was found that the generic critical properties were not in the universality class of directed percolation. In fact, since the critical properties vary with the parameters, they are not even universal.

The standard time evolution of a coupled-map-lattice is by synchronous (or parallel) updating, in which all individual maps of the lattice are iterated forward simultaneously in a completely deterministic way [8]. However, recently it was observed that the critical properties of a standard CML, using coupled logistic maps, depend crucially on the updating rules: when the dynamics in a two dimensional system was changed from “synchronous” to “asynchronous” the corresponding critical properties also changed [12]. Here, asynchronous means that in each step a random site on the CML is chosen and is iterated forward. In this case it was found [12] that the critical properties are universal and fall in the $2d$ Ising universality class.

In this letter, we apply the asynchronous updating to the coupled-map-lattice of spatio-temporal intermittency discussed above. We find that all critical exponents, independent of the choice of parameters, fall into the universality class of directed percolation. All critical characteristics of DP, such as hyper-scaling, are fulfilled, leading to independent controls of the values of the critical exponents. We believe that this resolves a long-standing puzzle of the relation between directed percolation and the dynamics of STI.

The original dynamics of the coupled-map-lattice of Chaté and Manneville [2] for a lattice with one space- and one time-direction is written in terms of a field $u_i(t)$ at site i and time t as

$$u_i(t+1) = f(u_i(t)) + \frac{\epsilon}{2} \Delta_f u_i(t), \quad (1)$$

where $\Delta_f u_i(t) = f(u_{i-1}(t)) - 2f(u_i(t)) + f(u_{i+1}(t))$. The parameter ϵ measures the strength of the coupling from site i to its two neighbours. The dynamics (1) is parallel or synchronous: all sites are updated at the same time.

The local map f is of the form:

$$f(x) = \begin{cases} rx, & \text{if } x \in [0, 1/2]; \\ r(1-x), & \text{if } x \in [1/2, 1]; \\ x, & \text{if } x \in [1, r/2]. \end{cases} \quad (2)$$

The chaotic motion of f for $x \leq 1$ is governed by a standard tent map of slope r . However, when r exceeds the value two, the trajectory may escape to a “laminar” state with $x > 1$, and this state is marginally stable, because the slope in the line of fixed points is one. As mentioned above, the laminar state is absorbing, i.e. the trajectory cannot be pulled back into the chaotic state. This is no longer the case, when the maps are coupled, since the interactions with its neighbours may pull a laminar site back into chaotic motion, thus causing the interesting interplay between laminar and turbulent regions.

In this work we consider the same CML under asynchronous updating: at time t a random site i_r is selected and is altered according to (1) while all the other variables keep their values:

$$\begin{aligned} u_{i_r}(t + 1/L) &= f(u_{i_r}(t)) + \frac{\epsilon}{2} \Delta_f u_{i_r}(t), \\ u_i(t + 1/L) &= u_i(t) \quad \text{for } i \neq i_r, \end{aligned} \quad (3)$$

where L is the size of the system. Note that with this choice of time step on average each site is updated once in one unit of time.

Fig. 1 shows a pattern generated in this way. As only one site is updated at a time, a new horizontal line in the time axis is added only after $L = 128$ time steps (i.e. $t \rightarrow t + 1$). We observe that the turbulent sites (black in Fig. 1) percolate through the system, sometimes ending in a dangling bond. The boundaries of these penetrating patterns are less regular than for the synchronous case [2]. In fact this type of pattern is closer to the experimentally observed STI patterns than the patterns generated with synchronous updating.

To estimate the critical exponents for the randomly updated CML (3), we follow the finite size scaling methods of Houlrik et al. [9–11]. First of all we have to locate the critical line in the parameter plane (ϵ, r) . This is done by measuring the absorption time $\tau(r, \epsilon, L)$, i.e. the time it takes the system starting from a random initial state to reach the absorbing state - averaged over an ensemble of initial conditions. At the critical point $\epsilon = \epsilon_c(r)$, this time diverges like

$$\tau(\epsilon_c, L) \sim L^z \quad (4)$$

where the usual dynamical exponent $z = \nu_{\parallel}/\nu_{\perp}$ has been introduced. Fig. 2 shows the phase diagram with the critical line and contrasts it with the critical line for the synchronously updated system (1) taken from [9]. We consider three different values of r and the corresponding values of ϵ_c and z are found in Table I.

The order parameter $m(\epsilon, L, t)$ is defined as the fraction of turbulent sites in the lattice, again averaged over many different initial states [9]. The order parameter scales in the usual way when approaching the critical line from above

$$m \sim (\epsilon - \epsilon_c)^{\beta} \quad \text{for } \epsilon \rightarrow \epsilon_c^+ \quad (5)$$

Using this relation we have estimated the β -exponent directly and the results are found in Table I. Applying finite-size scaling arguments we find the following scaling form at the critical point

$$m(\epsilon_c, t, L) \sim L^{-\beta/\nu_\perp} g(t/L^z). \quad (6)$$

The function $g(t/L^z)$ has the following properties: At times much smaller than the absorption time, one expects a power-law decay in time due to critical correlations and the L -dependent pre-factor in (6) must drop out. For $t \ll L^z$, we therefore have

$$m(\epsilon_c, t, L) \sim t^{-\beta/\nu_\parallel} \quad (7)$$

For times much larger than the absorption time, we may assume uncorrelated decay of the order parameter, and therefore the function g , will decay exponentially. Fig. 3 shows a plot of $m(\epsilon_c, t, L)$ versus t at $r = 2.2$. The curves for 7 different system sizes in the interval $L = 2^4, \dots, 2^{10}$ fall very accurately on the same line in the double logarithmic plot allowing determination of β/ν_\parallel as listed in Table I. As we see in this table all the critical exponents are, within the error bars, consistent with the values for directed percolation, listed at the bottom line in Table I.

In order to obtain independent checks on the values of the critical exponents we have performed a rescaling analysis using (6). The rescaled curves are shown in Fig. 4. For systems sizes in the interval $L = 2^4, \dots, 2^{10}$ the rescaled curves collapse very accurately to a single curve. The corresponding values of β/ν_\perp and z are shown in Table II- again consistent with DP.

To extract further critical exponents and to check hyper-scaling we have looked at the spatial correlations. Even though any dynamics of this CML will end up in the absorbing (laminar) state, it is possible to find non-trivial spatial correlations in a long lasting quasi stationary situation [10]. The correlations can be obtained from the pair correlation function

$$C_j(t) = \frac{1}{L} \sum_{i=1}^L \langle u_i(t) u_{i+j}(t) \rangle - \langle u(t) \rangle^2, \quad (8)$$

where the brackets denote the average over different initial conditions. If the coupling between the sites is weak, i.e. if ϵ is small, one might expect the spatial correlations to fall off exponentially with distance. At criticality, on the other hand, one expects an algebraic decay of correlations [10]

$$C_j(t) = j^{1-\eta} \psi(j/\xi(t)), \quad (9)$$

where η is the associated critical exponent, and correlations are induced over a length scale $\xi(t) \sim t^{1/z}$ as the CML relaxes towards a steady state. The (equal time) correlation function for various times (at $r = 2.2$) is shown in Fig. 5, indicating an algebraic decay in space after long time. The corresponding value of η from this direct measurements is shown in Table I together with values obtained at other r -values. Again the agreement with DP is confirmed.

For the spatial correlations, a rescaling analysis can also be performed by plotting $j/t^{1/z}$ versus $j^{\eta-1} C_j(t)$. Fig. 6 shows the corresponding rescaled plot and this technique allows another independent determination of z and η , the values of which are shown in Table II.

The fourth column of Table II contains the values of η obtained from the hyper-scaling relation

$$2\beta/\nu = d - 2 + \eta, \quad (10)$$

giving a third way of estimating the exponent η . All three ways of finding η give results that, within errorbars, are in agreement with the directed percolation value 1.51.

We thus conclude that our numerics gives very strong evidence for the fact that spatio-temporal intermittency in the form of asynchronous coupled maps falls in the universality class of directed percolation. The reason why synchronously updated maps do not behave in a universal way must thus be sought in the complicated correlations built up by the strong constraint of exactly simultaneous, completely deterministic updating, which, in most applications will not be fulfilled. Thus, experiments showing spatio-temporal intermittency should be describable by directed percolation near the transition to turbulence.

ACKNOWLEDGMENTS

J.R. gratefully acknowledges financial support by the Studienstiftung des deutschen Volkes.

REFERENCES

- [1] H. Chaté in *Spontaneous Formation of Space-Time Structures and Criticality*, ed. by T. Riste and D. Sherrington, p. 273 (Kluwer 1991).
- [2] H. Chaté and P. Manneville, Physica D **32**, 409 (1988).
- [3] H. Chaté and P. Manneville, Physica D **37**, 33 (1989).
- [4] Y. Pomeau, Physica D **23**, 3 (1986).
- [5] S. Ciliberto and P. Bigazzi, Phys. Rev. Lett. **60**, 286 (1988)
- [6] F. Daviaud, M. Dubois and P. Bergé, Europhys. lett. **9**, 441 (1989)
- [7] M. Rabaud, S. Michalland and Y. Couder, Phys. Rev. Lett. **64**, 184 (1990)
- [8] K. Kaneko, ed. *Theory and applications of coupled map lattices*, (Wiley 1993).
- [9] J. M. Houlrik, I. Webman and M. H. Jensen, Phys. Rev. A **41**, 4210 (1990)
- [10] J. M. Houlrik and M. H. Jensen, Phys. Lett. A **16**, 3275 (1992)
- [11] J. M. Houlrik and M. H. Jensen in *Theory and applications of coupled map lattices*, ed. by K. Kaneko, p. 95 (Wiley 1993).
- [12] P. Marcq, H. Chaté and P. Manneville, Phys. Rev. Lett. **77**, 4003 (1996)

FIGURES

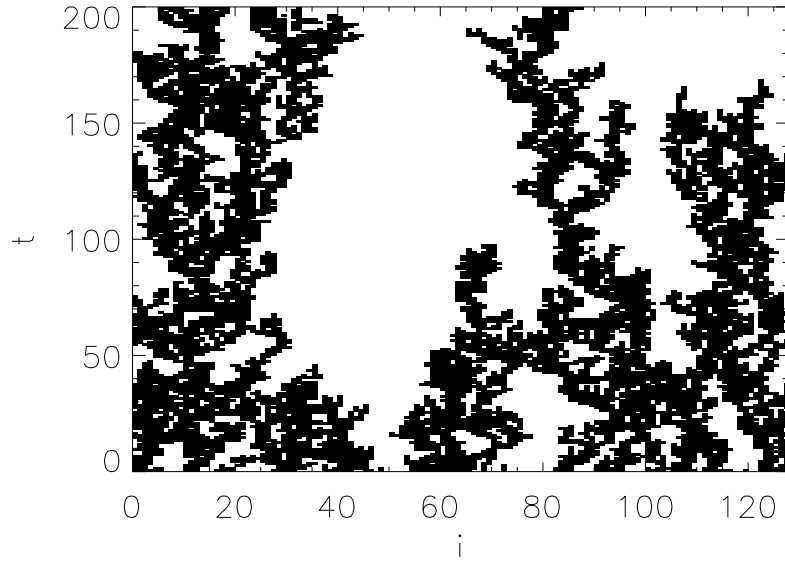


FIG. 1. Time evolution of the asynchronous CML (3) with $r = 3.0$, $\epsilon = 0.58$ and system size $L = 128$. The turbulent sites with $u \leq 1$ are black while the laminar sites with $u > 1$ are white.

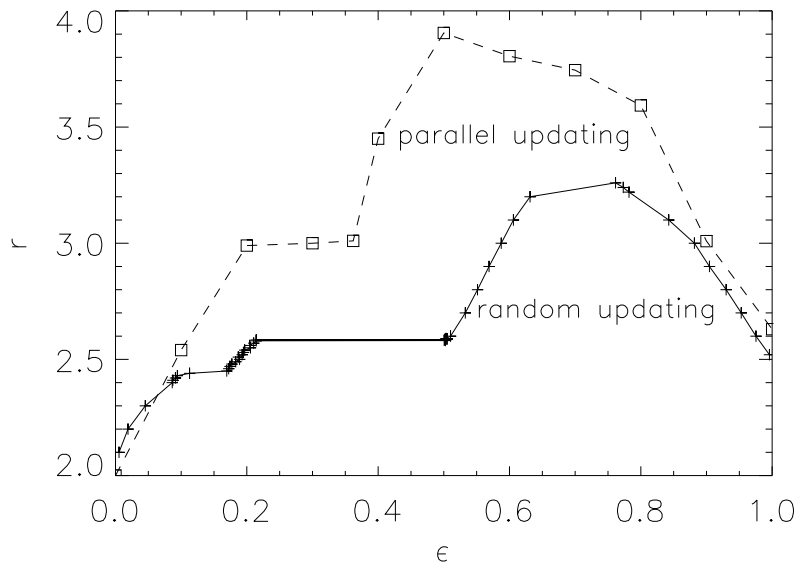


FIG. 2. Phase diagrams of one-dimensional CML for asynchronous updating (crosses) and synchronous updating (boxes).

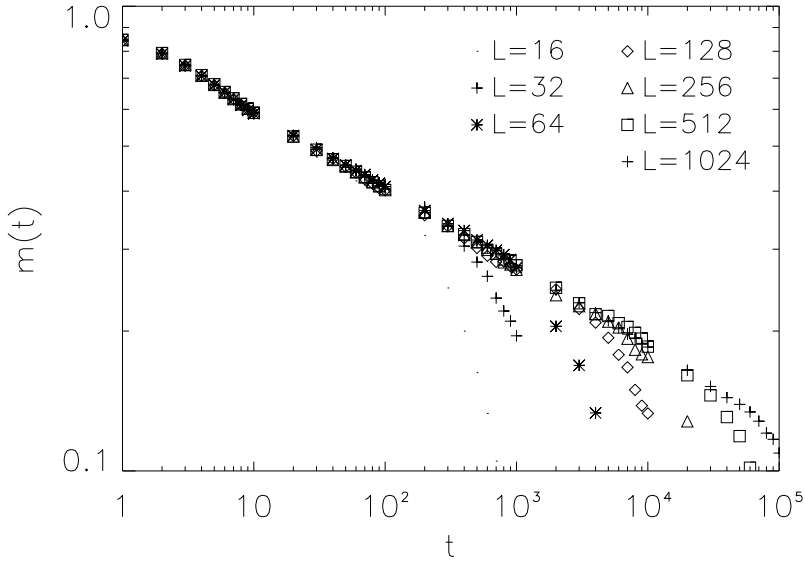


FIG. 3. Order parameter $m(t)$ versus time t for system sizes L between 2^4 and 2^{10} at $r = 2.2$. As expected the data falls on one line as long as t is much smaller than the escape time.

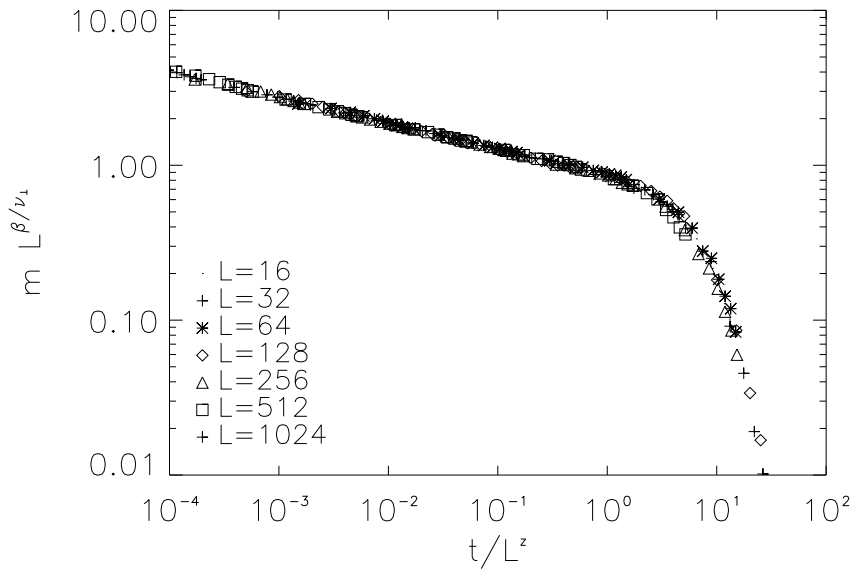


FIG. 4. Rescaling of the order parameter at $r = 2.2$ according to (6) to obtain estimates for β/ν_1 and for z . Data for for system sizes L between 2^4 and 2^{10} collapses on one curve.

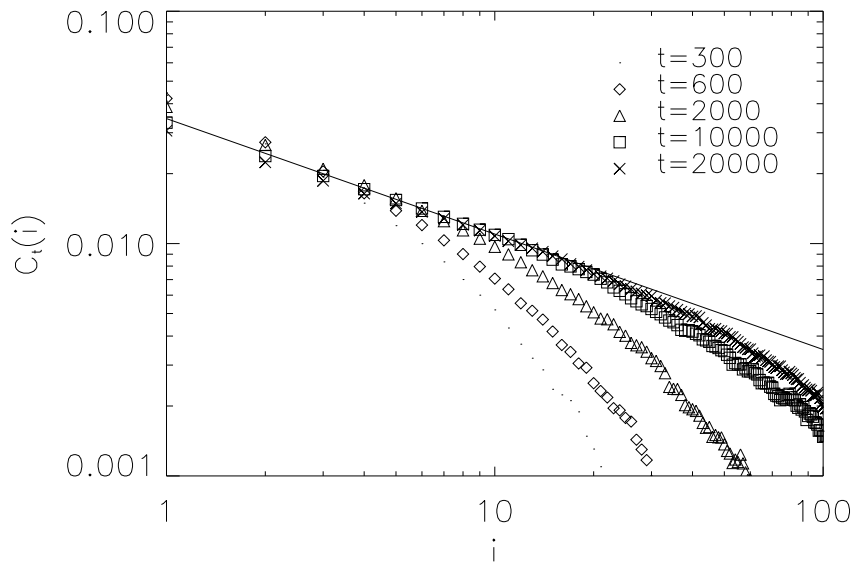


FIG. 5. Spatial correlation function $C_i(t)$ for various times t at $r = 2.2$. $C_i(t)$ approaches a straight line with slope $1 - \eta$ for large times, indicating an algebraic decay.

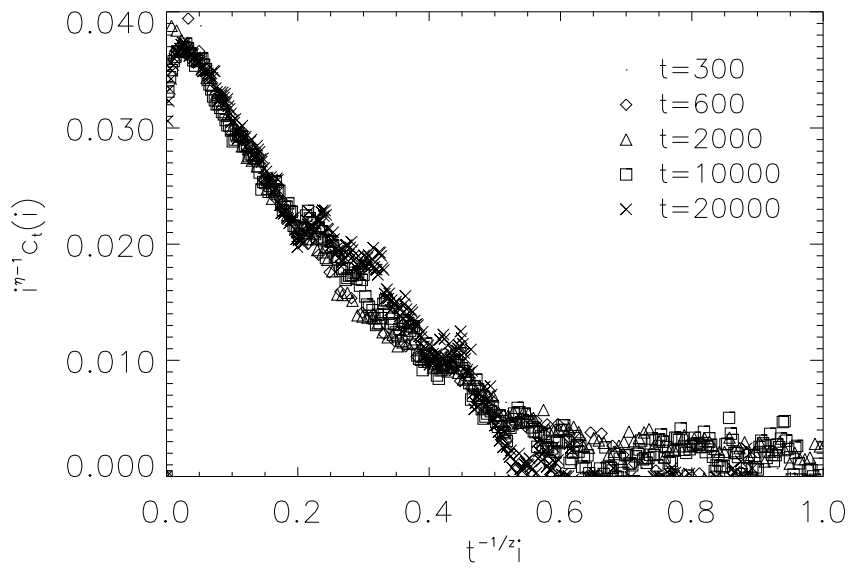


FIG. 6. Rescaled spatial correlation function at $r = 2.2$. The data for various times collapses on one curve if the exponents z and η take the values in table II.

TABLES

TABLE I. Direct measurements of the critical exponents for system (3). The critical values ϵ_c and the exponent z are found simultaneously by approaching the value of ϵ where the scaling (4) is best. The estimation of the other exponents are described in the text. The bottom line are the directed percolation exponents.

r	ϵ_c	z	β	$\frac{\beta}{\nu_{\parallel}}$	η
2.2	0.0195(2)	1.58(2)	0.28(1)	0.16(1)	1.51(2)
2.6	0.5096(2)	1.59(2)	0.28(1)	0.16(1)	1.49(2)
3.0	0.5870(3)	1.60(3)	0.28(1)	0.15(2)	1.50(2)
DP		1.57	0.28	0.16	1.51

TABLE II. The exponents and relations obtained from rescaling analysis using finite size scaling. The fourth column is an estimate of η using the hyper-scaling relation (10).

r	$\frac{\beta}{\nu_{\perp}}$	z	$\eta = 2\frac{\beta}{\nu_{\perp}} + 1$	z	η
2.2	0.26(1)	1.57(1)	1.52(2)	1.56(2)	1.53(2)
2.6	0.26(1)	1.57(1)	1.52(2)	1.58(2)	1.49(2)
3.0	0.25(2)	1.58(1)	1.50(3)	1.58(2)	1.53(2)
DP	0.26	1.57	1.51	1.57	1.51